Extended Synaptotagmin-1 Interacts With Protein Kinase A to Modulate β-Adrenergic Signaling and Cardiac Contractility

Shi-Hui WANG[1,2]*, Su-Huai WANG[3]*, Jia LI[1], Bo-Le CHEN[1], Ting-Yuan CHEN[1], Jia-Kun ZHANG[1], Lin SUN[1,2], Jing-Jie LI[1,2]

** These authors contributed equally to this work.*

[1]Department of Cardiology, The First Affiliated Hospital, Harbin Medical University, Harbin, China, [2]Central Laboratory of The First Affiliated Hospital Harbin Medical University, Harbin, China, [3]Department of Cardiology, Inner Mongolia Medical University Affiliated Hospital, Hohhot, China

Received February 28, 2026
Accepted June 16, 2026

Summary

Sympathetic activation of the heart enhances myocardial contractility *via* the β-adrenergic receptor/adenylate cyclase/cAMP/PKA signaling pathway. Although Protein Kinase A Catalytic Subunit (PKAc) mediates downstream protein phosphorylation, the mechanisms governing its subcellular localization remain unclear. Extended synaptotagmin-1 (E-Syt1), a stress-activated membrane tethering protein located at endoplasmic reticulum-plasma membrane (ER-PM) contact sites, has been associated with compartmentalization signals. This study aimed to investigate whether E-Syt1 modulates β-adrenergic signaling and cardiac contractility by coordinating the localization and activity of PKAc. Mice were injected the β-adrenergic agonist isoproterenol (ISO), and cardiac function was evaluated by echocardiography in E-Syt1 knockout (E-Syt1$^{-/-}$) and wild-type mice. E-Syt1 knockout mice exhibit reduced cardiac contractility after ISO treatment. Despite gene expression of the β-adrenergic pathway was not altered, ISO stimulation in E-Syt1$^{-/-}$ hearts resulted in reduced cytosolic cAMP levels and decreased phosphorylation of Cav1.2. LC-MS/MS and immunofluorescence verified the interaction between E-Syt1 and PKAc. Rescue experiments highlighted the critical role of E-Syt1-PKAc in mediating Cav1.2 phosphorylation through the SMP domain interactions. E-Syt1 regulates Cav1.2 phosphorylation by forming a signaling complex with PKAc, supporting efficient β-adrenergic signaling.

Key words

E-Syt1 • Protein kinase A • Cav1.2 • β-adrenergic signaling pathway • Sympathetic stimulation

Corresponding authors

J.-J. Li and L. Sun, Department of Cardiology, The First Affiliated Hospital of Harbin Medical University, Postal Street 23#, Nangang District, Harbin City, Heilongjiang Province, China. E-mail: circulation9999@163.com (J.-J. L.); drsunlin@sina.com (L. S.)

Introduction

During the "fight-or-flight" response, the sympathetic nervous system enhances myocardial contractility by activating the adenylyl cyclase (AC)-cAMP-protein kinase A (PKA) signaling cascade [1], which phosphorylates ion channel proteins [2]. Upon sympathetic stimulation, cAMP levels in cardiomyocytes do not increase uniformly throughout the cell but instead form multiple microdomains. These microdomains precisely regulate PKA activity by maintaining cAMP concentrations within nanodomains, promoting targeted phosphorylation of PKA substrates [3-5]. Cav1.2, the major subunit of cardiac L-type calcium channels, is a critical pathway for Ca^{2+} influx in cardiomyocytes. In the heart, activated PKAc predominantly phosphorylates the Ser1928 site of Cav1.2 in response to β-adrenergic stimulation, which is essential for triggering myocardial contraction [6]. Previous studies have shown that the

 An open access article under the CC BY 4.0 license https://creativecommons.org/licenses/by/4.0/ © 2026 by the authors. Published by the Institute of Physiology, Czech Academy of Sciences, Prague, Czech Republic. E-mail: physres@fgu.cas.cz, www.biomed.cas.cz/physiolres

signaling complex comprising PKA and Cav1.2 is localized within cAMP microdomains, facilitating efficient phosphorylation by PKA [7-10]. However, the mechanism by which PKAc is targeted to specific subcellular regions to regulate these signaling events remains unclear.

In cardiomyocytes, highly ordered endoplasmic reticulum-plasma membrane (ER-PM) microdomains are critical for maintaining signal transduction and gating of ion channels. The dynamic remodeling of these microdomains is mediated by intracellular tethering proteins. Here, we investigated E-Syt1, a newly identified stress protein in yeast [11] and non-excitable cells [12-14], which is in an autoinhibited state anchored to the endoplasmic reticulum (ER) at rest and is activated to recruit to the plasma membrane (PM) forming local microdomains upon stress [15,16]. In hepatocellular carcinoma cells, E-Syt1 can recruit PKCδ to the ER-PM and directly bind to PKCδ, affecting downstream signaling [17]. Similarly, in glioblastoma, E-Syt1 interacts with the GPR133 receptor, influencing submembrane cAMP dynamics [18].

Previous studies have demonstrated that certain scaffolding proteins can enhance the efficiency of cAMP/PKA signaling by generating intracellular signaling microdomains [19-23]. In the heart, PKA exists as a tetrameric holoenzyme in its inactive form, comprising two regulatory (R) and two catalytic (C) subunits. Four genes encode the regulatory subunits (RIα, RIβ, RIIα, and RIIβ), and three encode the catalytic subunits (Cα, Cβ, and Cγ), the latter conferring PKA's enzymatic activity. In the absence of cAMP, the R subunit dimer binds and inhibits the activity of the two C subunits. Upon an increase in cAMP levels, cAMP binds to the R subunits, inducing conformational changes and releasing the inhibition on the C subunit, allowing PKA to phosphorylate its targets [9,24]. The extensively studied PKA-binding proteins, A-kinase anchoring proteins (AKAPs), generally prefers to bind to type I and/or type II PKA. In the present study, LC-MS/MS analysis of enriched E-Syt1 extracted from cardiac tissue revealed that E-Syt1 primarily interacts with PKAc. We hypothesize that in the heart, E-Syt1 is activated in response to sympathetic stimulation and interacts with PKAc to form a signaling domain, promoting the specific phosphorylation of Cav1.2 by PKAc, thereby regulating the β-adrenergic signaling pathway.

Materials and Methods

Mouse models

All animal experiments were performed in accordance with the "Guidelines for the Care and Use of Laboratory Animals" and approved by the Institutional Animal Care and Use Committee (IACUC) of Harbin Medical University (Ethics Approval Number: 2022128). All procedures also complied with the current NIH guidelines for the protection of animals used in scientific research. Healthy male C57BL/6 mice were obtained from the Laboratory Animal Center of Harbin Medical University. The E-Syt1$^{-/-}$ mouse model on the C57BL/6 background was generated using CRISPR/Cas9 gene-editing technology and purchased from Suzhou Saiye Biotechnology Co., Ltd. All mice were housed individually under a 12 h light/dark cycle with free access to standard chow and water. Mice reached an average body weight of approximately 25 g at 7-8 weeks of age, and age-matched mice were randomly assigned to the experimental groups. Sympathetic nervous system stimulation was simulated by intraperitoneal injection of isoproterenol (5 mg/kg; II0200, Solarbio). At the end of the experiments, mice were euthanized by cervical dislocation, and heart tissues were collected for RNA-Sequencing analysis and subsequent biochemical analyses.

Echocardiography

Following intraperitoneal injection of 2.5 % avertin anesthesia, mice in the ISO group received a single intraperitoneal injection of isoproterenol (5 mg/kg), while control mice received an equal volume of saline. Based on our preliminary RT-qPCR results showing that E-Syt1 mRNA expression peaked at 1 h after isoproterenol administration, echocardiographic examination was performed 1 h after injection using the Vevo 2000 high-resolution small animal ultrasound imaging system in two-dimensional M-mode. The body temperature was maintained between 36.9 °C and 37.3 °C, and the heart rate was stabilized between 400 and 550 beats per minute. At the target heart rate, measurements of end-diastolic and end-systolic interventricular septum thickness, posterior wall thickness, and left ventricular internal diameter were obtained. Four consecutive cardiac cycles were analyzed using the manufacturer's software to calculate the left ventricular ejection fraction (LVEF) and fractional shortening (FS). FS and LVEF were calculated from M-mode measurements using standard formulas implemented in the Vevo 2000 software. LVEDV and LVESV

were estimated using the Teichholz method. All echocardiographic measurements were performed by an experienced researcher who was blinded to the experimental groups.

Isolation and culture of primary cardiomyocytes

Hearts from neonatal E-Syt1$^{-/-}$ mice (1-2 days old) were excised and placed in a pre-cooled DMEM medium. The atria were removed, and the ventricle was mince into uniform 1-2 mm^2 fragments, which were digested in trypsin solution (volume approximately twice that of the tissue). After centrifugation and resuspension, cells were plated and cultured in a incubator (5 % CO_2, 95 % humidity, 37 °C). After 90 min, a differential method was used to separate fibroblasts and cardiomyocytes. The cells were considered ready for subsequent experiments when they exhibited good morphology under microscope (see the Supplementary Materials for detailed procedures).

Cell transfection

Construct plasmids encoding full-length E-Syt1 (F: ACCGGTCGACATGGAGCGATCTCCAGGAGA; R: ACCGCCGCGGGGAGCTGCCCTTGTCCTTGT) and E-Syt1 mutants within the SMP domain (F: TACGATCGC AATGGAGCGATCTCCAGGA; R: TACGATCGTCAGG TAGAGGGCGAGGC). Add the plasmid (2000 μg) and Lipofectamine 2000 separately to the Opti-MEM, and incubate for 5 min. Mix these two liquids in the same EP tube, and add them to the cells 20 min later. After 48 h, transfection efficiency and cell morphology were evaluated before subsequent treatments.

Immunofluorescence staining

Cardiomyocytes were fixed with 4 % paraformaldehyde for 20 min, washed three times with PBS, and permeabilized with 1 % Triton X-100 for 10 min. After washing, cells were blocked with 10 % goat serum containing 1 % BSA for 1 h at room temperature. Cells were then incubated overnight at 4 °C with primary antibodies: rabbit anti-E-Syt1 (ABclonal, A15410) and mouse anti-PKAc (Invitrogen, MA5-31865). After washing, cells were incubated for 1 h at room temperature with secondary antibodies – Alexa Fluor 488-conjugated goat anti-rabbit IgG (H+L) ((Beijing Zhongshan Jinqiao Biotechnology Co., Ltd., ZF0311) and Alexa Fluor 594 goat anti-mouse IgG (H+L) (Beijing Zhongshan Jinqiao Biotechnology Co., Ltd., ZF0511). Images were acquired using an immunofluorescence microscope (Leica, Germany), and fluorescence intensity was quantified using ImageJ software.

Western blot (WB)

Protein extraction and Western blotting were performed following standard protocols. Primary antibodies used included anti-E-Syt1 (1:1000, ABclonal, A15410), anti-PKAc (1:1000, Invitrogen, MA5-31865), anti-ADRB1 (1:1000, Sigma, SAB2100064), anti-GNAS (1:1000, Invitrogen, PA5-19315), anti-adenylyl cyclase (1:1000, Abcam, ab66037), and anti-CaV1.2 (1:1000, Sigma, C124). Phospho-specific antibodies were used as previously described [8]. Anti-β-tubulin (1:1000, Santa Cruz, sc-166729) and anti-GAPDH (1:1000, Abcam, ab88425) were used as controls. The secondary antibodies were purchased from Beijing Zhongshan Jinqiao Biotechnology Co., Ltd. (see Supplementary Materials for detailed procedures).

Real-time quantitative polymerase chain reaction

Total RNA was extracted from heart tissue or cells using the Axy Prep Multisource Total RNA Mini-Prep Kit (AP-MN-MS-RNA-250, Axygen, USA). The total RNA was reverse transcribed into cDNA using the PrimeScript™ RT reagent Kit with gDNA Eraser (Perfect Real Time) (TAKARA, Japan). Real-time quantitative polymerase chain reaction (RT-qPCR) was performed for E-Syt1, ADRB1, GNAS, adenylate cyclase6, Prkaca, and Cacna1c using SYBR Green PCR master mix (A46012, ThermoFisher) and primers custom-designed by Applied Biosystems. After normalization with GAPDH, the relative expression levels of mRNA were calculated and quantified using the $2^{-\Delta\Delta CT}$ method (primer sequences available in Table S1).

Histological analysis

The mouse hearts were fixed in 4 % paraformaldehyde for 24 h, and embedded in paraffin., 4-5-μm-thick sections were cut and then stained with hematoxylin and eosin. The optical microscopic images were obtained using a Nikon E100 microscope.

LC-MS/MS and co-immunoprecipitation

Tissue or cell lysates were washed and centrifuged to collect the supernatant, to which 2 μg of E-Syt1 antibody was added. Non-specific immunoglobulin G (IgG) antibodies were included as a negative control. The samples were gently mixed overnight at 4 °C. Subsequently, 5 μl of Protein A/G Magnetic Beads were added to each sample and

mixed gently overnight at 4 °C. The samples were then sent to Oebioceth company in China for protein identification using LC-MS/MS. Following the same process before adding the beads, after overnight mixing at 4 °C, each sample was washed with 0.5 ml of Wash buffer, centrifuged again, and this washing step was repeated three times. After the final wash step, 50 µl of 1×SDS-PAGE Loading Buffer was added to the washed precipitate, mixed well, heated at 75 °C for 5 min, centrifuged at 800 rpm for 1 min, and the supernatant was collected for Western blot analysis.

ELISA for cAMP quantification

cAMP levels were quantified using an ELISA kit (CA201-1KT, Sigma) according to the manufacturer's protocol. Samples were heated at 95 °C for 40 min, cooled, and centrifuged at 4000 rpm for 10 min. The supernatant was collected, and absorbance was measured at 532 nm using a microplate reader.

Statistical analyses

Statistical analyses were performed using GraphPad Prism 8.0 software (GraphPad Software, Inc., La Jolla, CA, USA). Continuous variables were expressed as mean ± standard deviation (x±s). Data normality was assessed using the Shapiro-Wilk test. For normally distributed data, comparisons between two groups were performed using the independent sample *t*-test, and comparisons among multiple groups were conducted using one-way ANOVA. For non-normally distributed data, comparisons between two groups were carried out using the Mann-Whitney U test, and comparisons among multiple groups were conducted using the Kruskal-Wallis H test. A significance level of $P<0.05$ was considered statistically significant.

Results

Sympathetic stimulation upregulates E-Syt1, and E-Syt1 deletion reduces ISO-induced myocardial contractility

We first assessed E-Syt1 activation in wild-type (WT) mouse hearts following sympathetic stimulation. Heart tissues were collected at baseline and at 30 min, 1 h, 2 h, and 6 h after ISO administration for RT-qPCR analysis. E-Syt1 transcript levels peaked at 1 h post-ISO, significantly higher than the control group ($P<0.0001$) (Fig. 1A). We constructed an E-Syt1 knockout model (E-Syt1$^{-/-}$) based on C57BL/6 mice using CRISPR/Cas9 gene editing and successfully verified the knockout using Western Blot (WB) (Fig. 1B), with significantly increased expression after 1 h of iso administration (Fig. 1C). HE staining revealed no apparent pathological changes in E-Syt1$^{-/-}$ hearts under basal or ISO-stimulated conditions (Figure 1D). To further assess the impact of E-Syt1 on cardiac function, we conducted M-mode echocardiography on the four groups, focusing on key indicators including LVEF, LVFS, LVIDs, and LVIDd (Fig. 1E). M-mode echocardiography demonstrated that ISO significantly increased LVEF and LVFS in WT mice but not in E-Syt1$^{-/-}$ mice (Fig. 1E-F), indicating that E-Syt1 is required for the ISO-induced enhancement of myocardial contractility. Since ISO primarily activates β-adrenergic signaling, we next investigated whether E-Syt1 modulates this pathway during sympathetic activation.

Knocking out E-Syt1 did not alter β-adrenergic pathway gene expression but decreased ISO-induced intracellular cAMP increase

To delineate the molecular basis underlying the impaired contractile response in E-Syt1$^{-/-}$ mice, we performed transcriptomic sequencing of ISO and E-Syt1$^{-/-}$ + ISO-treated hearts. Compared with ISO group, 261 genes were upregulated and 255 were downregulated in E-Syt1$^{-/-}$+ ISO group (Fig. S1A, C). Functional enrichment analyses (COG, GO, KEGG) revealed no differentially expressed genes related to β-adrenergic signaling (Fig. S1B, D, E). RT-qPCR and Western blot analyses of Gnas (Gsα), Adcy6 (AC6), and Prkaca (PKAc) confirmed that E-Syt1 knockout did not alter their expression at either the mRNA or protein level across all experimental groups (Figs S2A-E, S3A-D). However, ELISA measurements showed that ISO significantly increased intracellular cAMP in WT hearts but not in E-Syt1$^{-/-}$ hearts (Fig. 2A). These findings indicate that E-Syt1 does not influence β-adrenergic gene expression, while it is essential for ISO-induced cAMP accumulation.

E-Syt1 modulates PKAc phosphorylation of CaV1.2 post-sympathetic stimulation

Given that E-Syt1 deletion reduced cAMP production without affecting β-adrenergic receptor or PKA gene expression, we hypothesized that E-Syt1 regulates local cAMP-PKA signaling microdomains. Western blot analysis showed that there was no difference in the total level of CaV1.2 protein among groups (Fig. 2B). However, ISO markedly enhanced CaV1.2 phosphorylation at Ser1928 (a known PKA target site) in WT but not in E-Syt1$^{-/-}$ hearts (Fig. 2C). These data suggest that E-Syt1 facilitates PKAc-dependent phosphorylation of CaV1.2 in response to sympathetic activation.

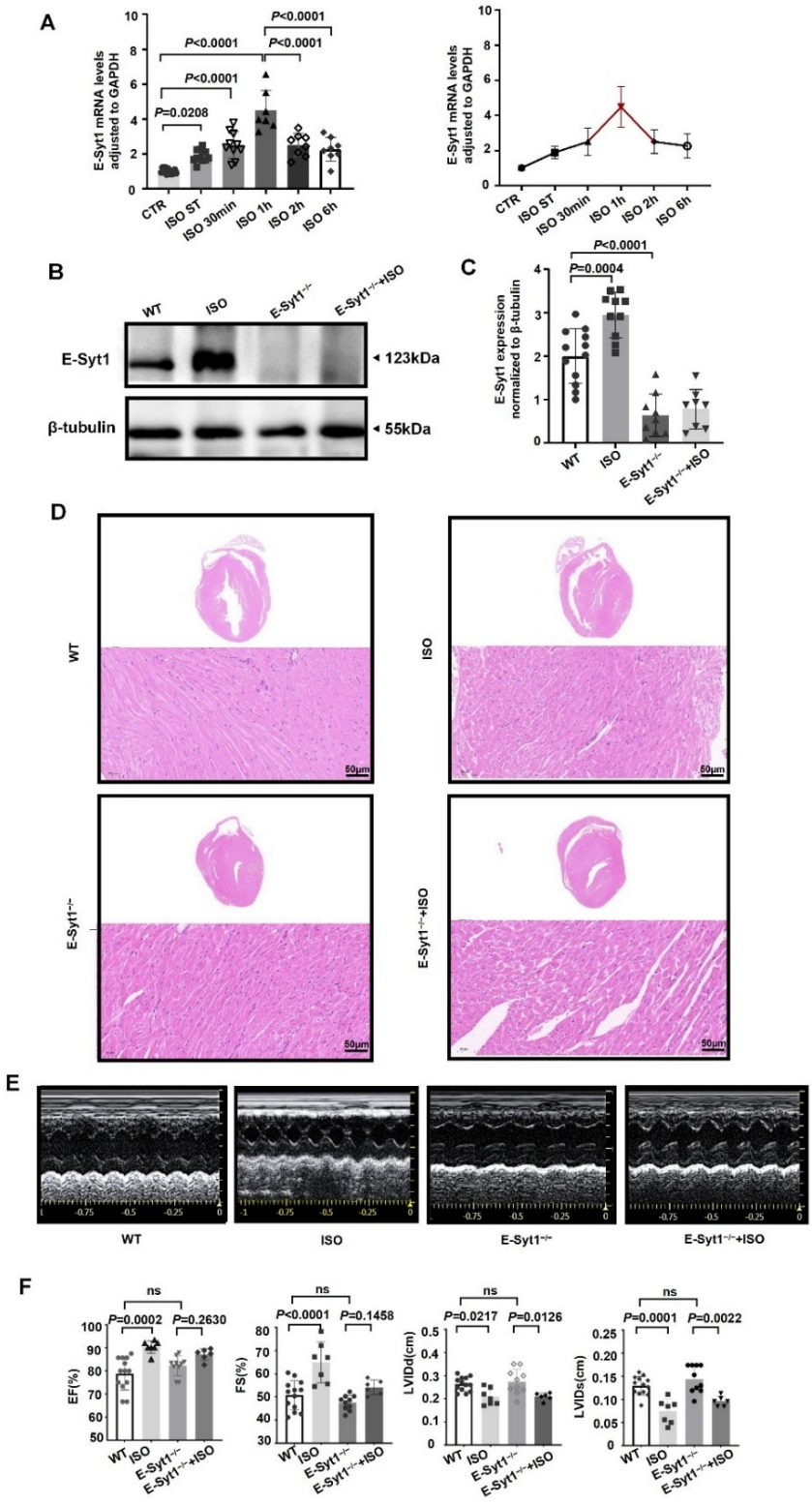


Fig. 1. Sympathetic stimulation upregulates E-Syt1, and E-Syt1 knockout reduces ISO-induced myocardial contractility. (**A**) PCR detects that E-Syt1 is activated after acute sympathetic stress, with the highest expression 1 h after ISO. (**B**) E-Syt1 knockout mice E-Syt1$^{-/-}$ were generated, and Western blot (WB) confirmed successful E-Syt1 knockout. (**C**) WB validates a significant increase in E-Syt1 expression 1 h after ISO. (**D**) Hematoxylin and eosin (HE) staining of heart sections to observe the structure and pathological changes in the hearts of Wild-type (WT), ISO, E-Syt1$^{-/-}$, and E-Syt1$^{-/-}$+ISO groups, Scale bar = 50 μm. (**E**) M-mode two-dimensional echocardiography evaluates the cardiac structure and function of the four groups of mice. (**F**) Inter-group cardiac echocardiographic evaluation, quantitative data including left ventricular ejection fraction (LVEF), left ventricular fractional shortening (LVFS), left ventricular end-diastolic dimension (LVIDd), and left ventricular end-systolic dimension (LVIDs). Data (A, C, and F) are expressed as mean ± standard deviation, compared using one-way analysis of variance, N=6-10 mice/group.

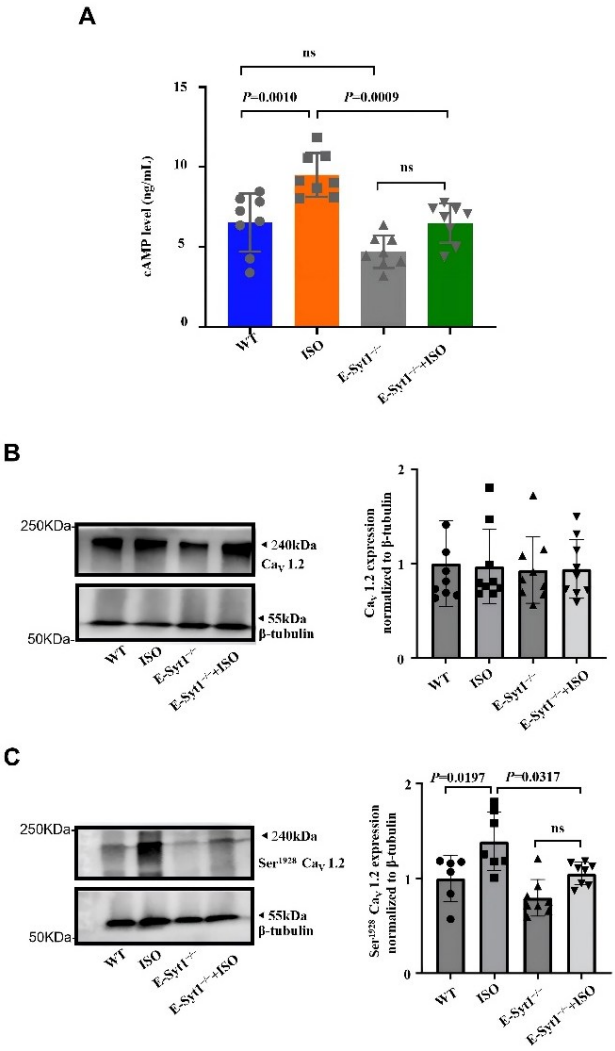


Fig. 2. Knocking out E-Syt1 reduces intracellular cAMP levels and expression of phosphorylated Cav1.2 channel at Ser1928 site after ISO. (**A**) Expression of cAMP levels in cardiac tissues of the WT, ISO, E-Syt1$^{-/-}$, and E-Syt1$^{-/-}$+ISO groups. (**B**) Cav1.2 protein expression, and (**C**) Ser1928 Cav1.2 protein expression. All data are presented as mean ± standard deviation, compared using one-way analysis of variance, N=6-10 mice/group.

E-Syt1 interacts with PKAc in cardiac tissue

To investigate how E-Syt1 affects PKAc substrate phosphorylation, we enriched E-Syt1 from myocardial tissues and conducted LC-MS/MS analysis, revealing PKAc as a potential E-Syt1 interacting partner (Fig. 3A). Co-immunoprecipitation (CO-IP) assays confirmed that ADRB1, Gsα, and AC6 did not pulled down with E-Syt1 (Fig. 3B), but PKAc did (Fig. 3C). This interaction was absent in E-Syt1$^{-/-}$ hearts (Fig. 3D). Immunofluorescence analysis of primary cardiomyocytes showed a significant increase in co-localization of E-Syt1 and PKAc after ISO treatment (Fig. 3E, F), further supporting their functional association in the β-adrenergic signaling cascade.

E-Syt1 interacts with PKAc via the SMP domain, impacting Cav1.2 phosphorylation after ISO

E-Syt1 has an N-terminal domain that anchors to the ER, an SMP (synaptotagmin-like mitochondrial-lipid-binding protein) domain, and multiple C2 domains, which connect to the plasma membrane upon activation [25-27]. Based on its domain architecture, we hypothesized that the SMP domain mediates PKAc binding. To test this, primary cardiomyocytes isolated from neonatal E-Syt1$^{-/-}$ mice were transfected with either full-length E-Syt1 (KO+E-Syt1) or an SMP-deletion mutant KO+△SMP-E-Syt1). Western blot analysis confirmed successful transfection of the E-Syt1 plasmid (Fig. 4A) and showed no impact on the total amount of PKAc protein (Fig. 4B). CO-IP showed that PKAc co-precipitated with full-length E-Syt1 but not with ΔSMP-E-Syt1, even after ISO stimulation (Fig. 4C). These results indicate that E-Syt1 interacts with PKAc *via* the SMP domain.

Additionally, we found no significant differences in total Cav1.2 protein levels among the groups (Fig. 4D). Transfection with full-length E-Syt1 significantly increased phosphorylation levels of Cav1.2 at the Ser1928 site following ISO stimulation, whereas transfection with △SMP-E-Syt1 did not rescue the response to ISO (Fig. 4E).

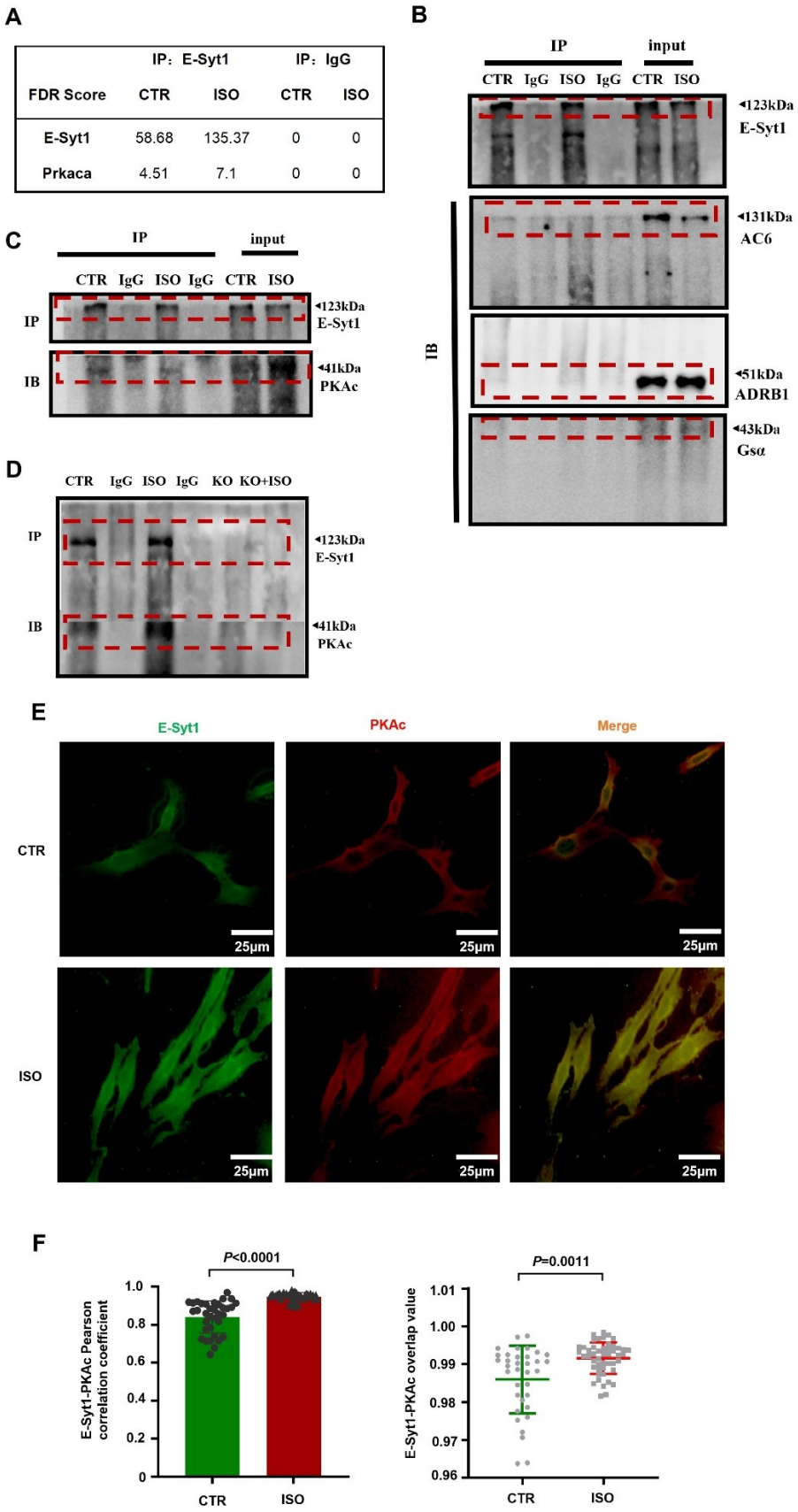


Fig. 3. E-Syt1 interacts with PKAc in the heart. (**A**) Results of LC-MS/MS analysis. (**B**) Immunoprecipitation (CO-IP) enrichment of ADRB1, Gsα, and AC6 after pulling down E-Syt1. (**C** and **D**) Pull-down of PKAc after enriching E-Syt1. (**E**) Immunofluorescence staining of cardiac myocytes, Scale bar = 25 μm. (**F**) Pearson correlation coefficient and overlap value of co-localization. Data (F) are presented as mean ± standard deviation and compared using independent samples *t*-test. N=10-20 cells/group.

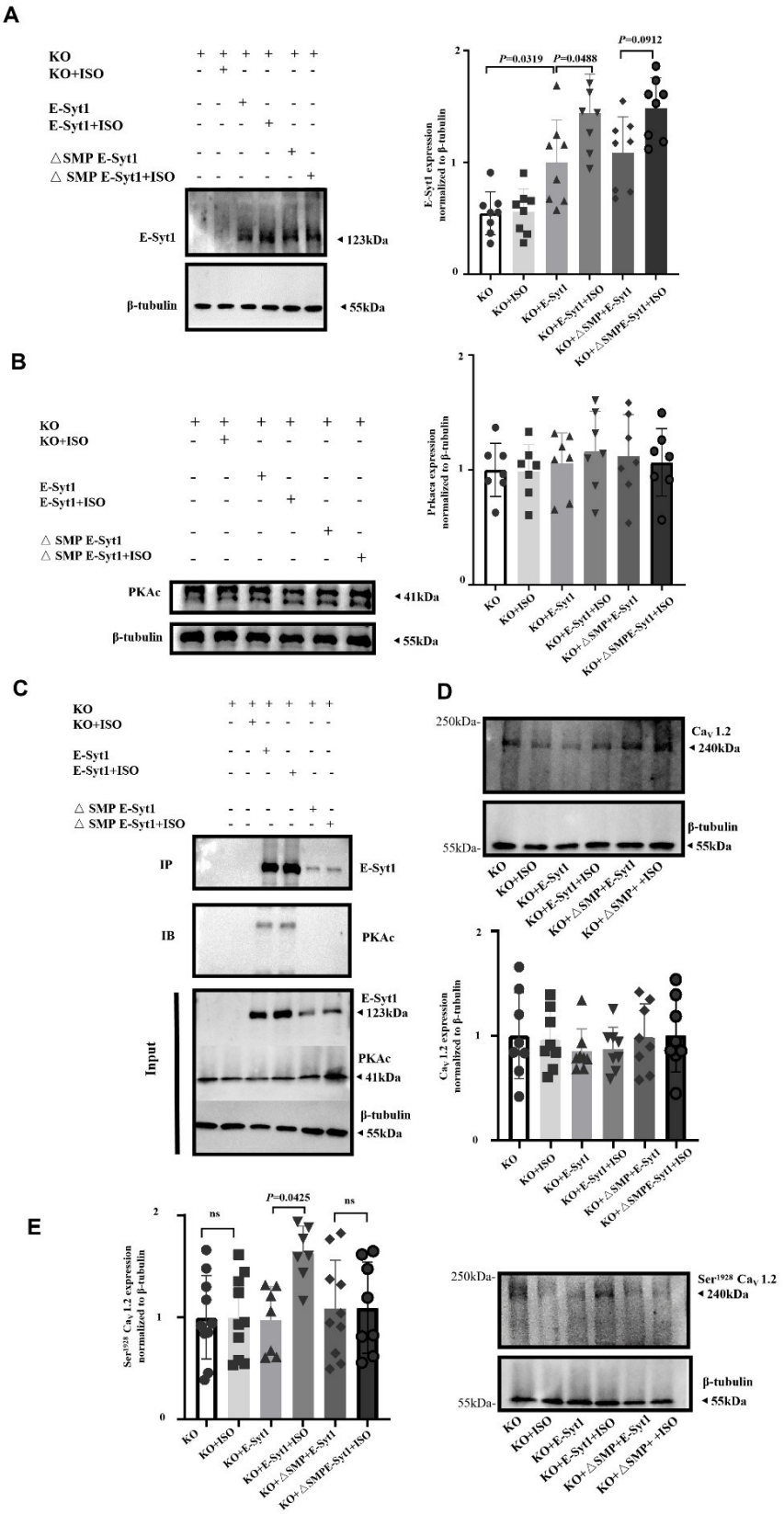


Fig. 4. E-Syt1 interacts with PKAc through the SMP domain, influencing the phosphorylation of $Ca_v1.2$ after ISO. Cardiac myocytes from E-Syt1$^{-/-}$ mice (knock-out, KO) were transfected with full-length E-Syt1 (KO+E-Syt1) and point-mutated E-Syt1 in the SMP domain (KO+△SMP-E-Syt1). (**A**) WB validates the expression of E-Syt1 protein in each group. (**B**) WB validates the expression of PKAc protein in each group. (**C**) CO-IP experiment confirms that E-syt1 pulls down PKAc through SMP domain. (**D**) WB validates the protein levels of $Ca_v1.2$ in each group. (**E**) WB validates the protein levels of Ser1928 $Ca_v1.2$ in each group. Data are presented as mean ± standard deviation and compared using one-way analysis of variance. N=5-10 cells/group.

Discussion

In this study, we identified E-Syt1 as a novel regulator of β-adrenergic signaling in the heart. E-Syt1 expression was significantly upregulated following ISO stimulation. Cardiac ultrasound revealed that myocardial contractility in E-Syt1$^{-/-}$ mice was significantly lower than in wild-type mice after ISO treatment. Mechanistically, E-Syt1 knockout reduced ISO-induced intracellular cAMP accumulation and PKAc-dependent phosphorylation of CaV1.2. LC-MS/MS analysis and CO-IP experiments revealed an interaction between E-Syt1 and PKAc, mediated through the SMP domain. Based on these findings, we propose a model in which sympathetic stimulation activates E-Syt1, promoting its translocation from the ER to the plasma membrane (PM). At the ER-PM junctions, E-Syt1 interacts with PKAc to form a local signaling domain that enables efficient subcellular phosphorylation of CaV1.2 by PKAc (Fig. 5).

Our findings highlight an essential role for E-Syt1 in modulating cAMP/PKA signaling at the subcellular level. Although transcriptomic analysis and PCR validation revealed no significant alterations in β1-adrenergic pathway gene expression in E-Syt1$^{-/-}$ hearts, ISO-induced cAMP production and Cav1.2 phosphorylation were markedly reduced. This suggests that E-Syt1 does not affect upstream β1-adrenergic receptor or adenylyl cyclase expression but instead influences the downstream signaling. Previous studies in non-cardiac cells have shown that E-Syt1 rapidly alters intracellular spatial substructures under stress [16,28,29]. For instance, in HEK293 cells, E-Syt1 participates in the reorganization of the ER to form a ring structure that encircles ion channels [30], while in Drosophila photoreceptor cells, E-Syt1 forms ER-PM platforms that ensure correct protein localization within the cell [31]. Combining ELISA results, we propose that sympathetic activation of E-Syt1 likely remodels spatial microdomains, thereby altering intracellular cAMP concentrations.

It is well established that PKA can be precisely localized to different subcellular locations, targeting the phosphorylation of ion channels, including cardiac Cav1.2 [3.4,9,23]. This compartmentalized cAMP/PKA signaling platform requires the participation of anchoring proteins [10,19-22,32,33], though the exact mechanisms remain incompletely defined. Through LC-MS/MS analysis, we identified a specific interaction between E-Syt1 and PKAc, which was further enhanced following ISO stimulation. Immunofluorescence staining confirmed this interaction, showing increased colocalization of E-Syt1 and PKA under sympathetic activation. Importantly, CO-IP experiments excluded direct interactions between E-Syt1 and other β1-adrenergic pathway proteins (ADRB1, Gsα, or AC6). Furthermore, in cardiac tissue from E-Syt1$^{-/-}$ mice, PKA is no longer pulled down, confirming that E-Syt1 activation enables the formation of a signaling complex with PKAc, facilitating the rapid and efficient phosphorylation of Cav1.2 under the stimulation of β-adrenergic receptors and the local increase of cAMP.

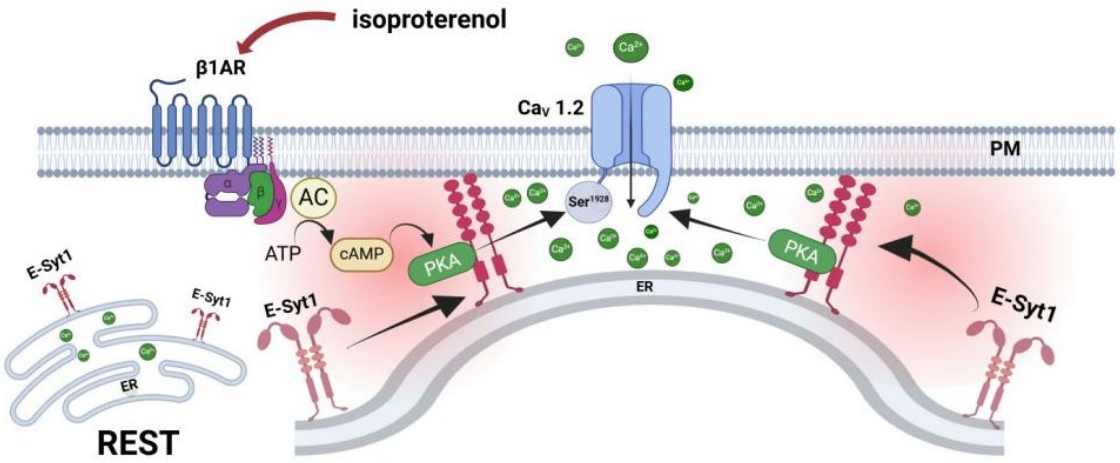


Fig. 5. E-Syt1 anchors to the endoplasmic reticulum (ER) in an inhibitory state at rest. Following sympathetic nervous system excitation, E-Syt1 is activated and recruited to the plasma membrane (PM), where it binds with PKAc to form a microdomain, facilitating efficient phosphorylation of $Ca_V1.2$ by PKAc in the subcellular space.

Considering the basic molecular structure of E-Syt1, including an N-terminal membrane anchor, an SMP domain, and multiple C2 domains [25-27], we know that the N-terminus functions as an anchor in the ER, while the C2 domains connect to the PM upon activation. Therefore, we hypothesized that the interaction between E-Syt1 and PKAc is likely to be mediated through the SMP domain. Supporting our hypothesis, recent studies have shown that the SMP domain mediates the interaction between E-Syt1 and proteins such as Sec22b in neurons [34] and Casp-11 in inflammasomes [35]. Rescue experiments using cardiomyocytes isolated from E-Syt1$^{-/-}$ neonatal mice and conducted *in vitro* transfection with the full-length E-Syt1 or E-Syt1 with point mutations in the SMP domain. These results further confirmed that the SMP domain is essential for E-Syt1-PKAc binding, as well as the subsequent phosphorylation of Cav1.2.

In cardiomyocytes, PKA is composed of two regulatory (R) and two catalytic (C) subunits. Our findings reveal that E-Syt1 primarily interacts with PKAc, which is different from AKAPs, the most extensively studied PKA-binding proteins. The AKAPs typically bind to either type I or type II PKA. AKAPs interact with the R subunit through amphiphilic helical residues and bind to the PKA-II subunit with nanomolar affinity [20]. E-Syt1 may serve as a novel class of PKA-anchoring molecules that function through a unique mechanism, which requires further study in the future.

Physiologically, β-adrenergic signaling pathway activated by sympathetic nerves can significantly increase intracellular calcium current through CaV1.2 channels [6], which is the basis for excitation-contraction coupling and cardiac contraction in cardiomyocytes [2,36]. However, excessive β-adrenergic activation can induce Ca^{2+} overload, contributing to arrhythmias [37-39]. Similar to β-blockers, which are contraindicated in acute heart failure patients due to their inhibition of myocardial contractility despite their anti-arrhythmic effects. In the mechanisms of heart disease, whether E-Syt1 is more involved in myocardial contractility or arrhythmogenesis requires further investigation. Our study provides potential targets for the localized manipulation of PKA signaling and drug delivery.

Conclusions

Our research has determined that E-Syt1 is a key molecule of β-adrenergic signaling in the heart. The specific interaction between E-Syt1 and the PKAc, which is essential for efficient ISO-triggered phosphorylation of CaV1.2. This interaction is mediated by the SMP domain of E-Syt1, influencing β-adrenergic regulation in the heart. Collectively, these findings define an E-Syt1-PKAc signaling axis that is responsible for the regional phosphorylation of CaV1.2 and for the fine regulation of the cardiac contraction response triggered by stress. This highlights the potential role of E-Syt1 as a target for PKA signal regulation in cardiovascular diseases.

Conflict of Interest

There is no conflict of interest.

Acknowledgements

This work was supported by the First Affiliated Hospital of Harbin Medical University [NO.2020IIT047 to J.J.L., Grant Nos.2023IIT129 to L.S] and Inner Mongolia Medical University Affiliated Hospital [NO.2026SHZR0193 to Su-Huai Wang].

Declaration of Generative AI and AI-Assisted Technologies in the Writing Process

The authors did not use generative AI or AI-assisted technologies in the development of this manuscript.

References

1. Lymperopoulos A, Rengo G, Koch WJ. Adrenergic nervous system in heart failure: pathophysiology and therapy. Circ Res 2013;113:739-753. https://doi.org/10.1161/CIRCRESAHA.113.300308
2. Mayourian J, Ceholski DK, Gonzalez DM, Cashman TJ, Sahoo S, Hajjar RJ, Costa KD. Physiologic, Pathologic, and Therapeutic Paracrine Modulation of Cardiac Excitation-Contraction Coupling. Circ Res 2018;122:167-183. https://doi.org/10.1161/CIRCRESAHA.117.311589
3. Lefkimmiatis K, Zaccolo M. cAMP signaling in subcellular compartments. Pharmacol Ther 2014;143:295-304. https://doi.org/10.1016/j.pharmthera.2014.03.008
4. Dodge-Kafka KL, Langeberg L, Scott JD. Compartmentation of cyclic nucleotide signaling in the heart: the role of A-kinase anchoring proteins. Circ Res 2006;98:993-1001. https://doi.org/10.1161/01.RES.0000218273.91741.30

5. Smith FD, Reichow SL, Esseltine JL, Shi D, Langeberg LK, Scott JD, Gonen T. Intrinsic disorder within an AKAP-protein kinase A complex guides local substrate phosphorylation. Elife 2013;2:e01319. https://doi.org/10.7554/eLife.01319
6. Ahern BM, Satin J. The L-type calcium channel current modulation mechanism: the plot thickens and fogs. J Clin Invest 2019;129:496-498. https://doi.org/10.1172/JCI125958
7. Navedo MF, Santana LF. CaV1.2 sparklets in heart and vascular smooth muscle. J Mol Cell Cardiol 2013;58:67-76. https://doi.org/10.1016/j.yjmcc.2012.11.018
8. Hall DD, Davare MA, Shi M, Allen ML, Weisenhaus M, McKnight GS, Hell JW. Critical role of cAMP-dependent protein kinase anchoring to the L-type calcium channel Cav1.2 via A-kinase anchor protein 150 in neurons. Biochemistry 2007;46:1635-1646. https://doi.org/10.1021/bi062217x
9. Torres-Quesada O, Mayrhofer JE, Stefan E. The many faces of compartmentalized PKA signalosomes. Cell Signal 2017;37:1-11. https://doi.org/10.1016/j.cellsig.2017.05.012
10. Wang L, Gamal El-Din TM, Catterall WA. AKAPs contribute to the indirect pathway for regulation of CaV1.2 channels by RAD and PKA. Biophys J 2024;123(Suppl 1):257a. https://doi.org/10.1016/j.bpj.2023.11.1617
11. Thomas FB, Omnus DJ, Bader JM, Chung GH, Kono N, Stefan CJ. Tricalbin proteins regulate plasma membrane phospholipid homeostasis. Life Sci Alliance 2022;5:e202201430. https://doi.org/10.26508/lsa.202201430
12. Idevall-Hagren O, Lü A, Xie B, De Camilli P. Triggered Ca2+ influx is required for extended synaptotagmin 1-induced ER-plasma membrane tethering. EMBO J 2015;34:2291-2305. https://doi.org/10.15252/embj.201591565
13. Giordano F, Saheki Y, Idevall-Hagren O, Colombo SF, Pirruccello M, Milosevic I, et al. PI(4,5)P(2)-dependent and Ca(2+)-regulated ER-PM interactions mediated by the extended synaptotagmins. Cell 2013;153:1494-1509. https://doi.org/10.1016/j.cell.2013.05.026
14. Chang CL, Hsieh TS, Yang TT, Rothberg KG, Azizoglu DB, Volk E, et al. Feedback regulation of receptor-induced Ca2+ signaling mediated by E-Syt1 and Nir2 at endoplasmic reticulum-plasma membrane junctions. Cell Rep 2013;5:813-825. https://doi.org/10.1016/j.celrep.2013.09.038
15. Bian X, Saheki Y, De Camilli P. Ca2+ releases E-Syt1 autoinhibition to couple ER-plasma membrane tethering with lipid transport. EMBO J 2017;37:219-234. https://doi.org/10.15252/embj.201797359
16. Saheki Y, Bian X, Schauder CM, Sawaki Y, Surma MA, Klose C, et al. Control of plasma membrane lipid homeostasis by the extended synaptotagmins. Nat Cell Biol 2016;18:504-515. https://doi.org/10.1038/ncb3339
17. Yamada K, Motohashi S, Oikawa T, Tago N, Koizumi R, Ono M, et al. Extended-synaptotagmin 1 engages in unconventional protein secretion mediated via SEC22B+ vesicle pathway in liver cancer. Proc Natl Acad Sci U S A 2022;119:e2202730119. https://doi.org/10.1073/pnas.2202730119
18. Stephan G, Haddock S, Wang S, Erdjument-Bromage H, Liu W, et al. Modulation of GPR133 (ADGRD1) signaling by its intracellular interaction partner extended synaptotagmin 1. Cell Rep 2024;43:114229. https://doi.org/10.1016/j.celrep.2024.114229
19. Sherpa RT, Moshal KS, Agarwal SR, Ostrom RS, Harvey RD. Role of protein kinase A and A kinase anchoring proteins in buffering and compartmentation of cAMP signalling in human airway smooth muscle cells. Br J Pharmacol 2024;181:2622-2635. https://doi.org/10.1111/bph.16357
20. Omar MH, Scott JD. AKAP Signaling Islands: Venues for Precision Pharmacology. Trends Pharmacol Sci 2020;41:933-946. https://doi.org/10.1016/j.tips.2020.09.007
21. Rababa'h A, Singh S, Suryavanshi SV, Altarabsheh SE, Deo SV, McConnell BK. Compartmentalization role of A-kinase anchoring proteins (AKAPs) in mediating protein kinase A (PKA) signaling and cardiomyocyte hypertrophy. Int J Mol Sci 2014;16:218-29. https://doi.org/10.3390/ijms16010218
22. Subramanian H, Nikolaev VO. A-Kinase Anchoring Proteins in Cardiac Myocytes and Their Roles in Regulating Calcium Cycling. Cells 2023;12:436. https://doi.org/10.3390/cells12030436
23. Yu H, Yuan C, Westenbroek RE, Catterall WA. The AKAP Cypher/Zasp contributes to β-adrenergic/PKA stimulation of cardiac CaV1.2 calcium channels. J Gen Physiol 2018;150:883-889. https://doi.org/10.1085/jgp.201711818
24. Marx SO, Reiken S, Hisamatsu Y, Jayaraman T, Burkhoff D, Rosemblit N, Marks AR. PKA phosphorylation dissociates FKBP12.6 from the calcium release channel (ryanodine receptor): defective regulation in failing hearts. Cell 2000;101:365-376. https://doi.org/10.1016/S0092-8674(00)80847-8

25. Wang Y, Li Z, Wang X, Zhao Z, Jiao L, Liu R, et al. Insights into membrane association of the SMP domain of extended synaptotagmin. Nat Commun 2023;14:1504. https://doi.org/10.1038/s41467-023-37202-8
26. Ge J, Bian X, Ma L, Cai Y, Li Y, Yang J, et al. Stepwise membrane binding of extended synaptotagmins revealed by optical tweezers. Nat Chem Biol 2022;18:313-320. https://doi.org/10.1038/s41589-021-00914-3
27. Schauder CM, Wu X, Saheki Y, Narayanaswamy P, Torta F, Wenk MR, et al. Structure of a lipid-bound extended synaptotagmin indicates a role in lipid transfer. Nature 2014;510:552-555. https://doi.org/10.1038/nature13269
28. Henry C, Carreras-Sureda A, Demaurex N. Enforced tethering elongates the cortical endoplasmic reticulum and limits store-operated Ca2+ entry. J Cell Sci 2022;135:jcs259313. https://doi.org/10.1242/jcs.259313
29. Hoffmann PC, Bharat TAM, Wozny MR, Boulanger J, Miller EA, Kukulski W. Tricalbins Contribute to Cellular Lipid Flux and Form Curved ER-PM Contacts that Are Bridged by Rod-Shaped Structures. Dev Cell 2019;51:488-502.e8. https://doi.org/10.1016/j.devcel.2019.09.019
30. Kang F, Zhou M, Huang X, Fan J, Wei L, Boulanger J, Liu Z, et al. E-syt1 Re-arranges STIM1 Clusters to Stabilize Ring-shaped ER-PM Contact Sites and Accelerate Ca2+ Store Replenishment. Sci Rep 2019;9:3975. https://doi.org/10.1038/s41598-019-40331-0
31. Nath VR, Mishra S, Basak B, Trivedi D, Raghu P. Extended synaptotagmin regulates membrane contact site structure and lipid transfer function in vivo. EMBO Rep 2020;21:e50264. https://doi.org/10.15252/embr.202050264
32. Huang T, Zhang B, Wang Z, Wang Y, Li W, Wang H. AKAP5 anchors PKA to enhance regulation of the HERG channel. Int J Biochem Cell Biol 2020;122:105741. https://doi.org/10.1016/j.biocel.2020.105741
33. Lygren B, Carlson CR, Santamaria K, Lissandron V, McSorley T, Litzenberg J, Lorenz D, et al. AKAP complex regulates Ca2+ re-uptake into heart sarcoplasmic reticulum. EMBO Rep 2007;8:1061-1067. https://doi.org/10.1038/sj.embor.7401081
34. Gallo A, Danglot L, Giordano F, Hewlett B, Binz T, Vannier C, Galli T. Role of the Sec22b-E-Syt complex in neurite growth and ramification. J Cell Sci 2020;133:jcs247148. https://doi.org/10.1242/jcs.247148
35. Ma Y, Zhao R, Guo H, Tong Q, Langdon WY, Liu W, Zhang J, et al. Cytosolic LPS-induced caspase-11 oligomerization and activation is regulated by extended synaptotagmin 1. Cell Rep 2023;42:112726. https://doi.org/10.1016/j.celrep.2023.112726
36. Bers DM. Cardiac excitation-contraction coupling. Nature 2002;415:198-205. https://doi.org/10.1038/415198a
37. Chung WH, Lin YN, Wu MY, Chang KC. Sympathetic Modulation in Cardiac Arrhythmias: Where We Stand and Where We Go. J Pers Med 2023;13:786. https://doi.org/10.3390/jpm13050786
38. Elsokkari I, Tsuji Y, Sapp JL, Nattel S. Recent Insights Into Mechanisms and Clinical Approaches to Electrical Storm. Can J Cardiol 2022;38:439-453. https://doi.org/10.1016/j.cjca.2021.12.015
39. Cauti FM, Rossi P, Sommer P. The sympathetic nervous system and ventricular arrhythmias: an inseparable union. Eur Heart J 2021;42:3588-3590. https://doi.org/10.1093/eurheartj/ehab168